ARTICLE IN PRESS
JID: JJBE [m5G;October 20, 2016;1:56]
Medical Engineering and Physics 000 (2016) 1–16
Contents lists available at ScienceDirect
Medical Engineering and Physics
journal homepage: www.elsevier.com/locate/medengphy

A computational assessment of the hemodynamic effects of crossed and non-crossed bifurcated stent-graft devices for the treatment of abdominal aortic aneurysms

Florian Stefanov[a], Tim McGloughlin[b], Liam Morris[a,*]

[a] Galway Medical Technologies Centre, Department of Mechanical and Industrial Engineering, Galway Mayo Institute of Technology, Galway, Ireland
[b] Department of Biomedical Engineering, Khalifa University, Abu Dhabi, United Arab Emirates

ARTICLE INFO

Article history:
Received 10 December 2015
Revised 22 August 2016
Accepted 23 September 2016
Available online xxx

Keywords:
Abdominal aortic aneurysms
Endovascular aneurysm repair
Stent-graft
Crossing/non-crossing
Geometrical parameters
Hemodynamics
Recirculations
Drag force
Spiral flow

ABSTRACT

There are several issues attributed with abdominal aortic aneurysm endovascular repair. The positioning of bifurcated stent-grafts (SG) may affect SG hemodynamics. The hemodynamics and geometrical parameters of crossing or non-crossing graft limbs have not being totally accessed. Eight patient-specific SG devices and four pre-operative cases were computationally simulated, assessing the hemodynamic and geometrical effects for crossed ($n=4$) and non-crossed ($n=4$) configurations. SGs eliminated the occurrence of significant recirculations within the sac prior treatment. Dean's number predicted secondary flow locations with the greatest recirculations occurring at the outlets especially during the deceleration phase. Peak drag force varied from 3.9 to 8.7 N, with greatest contribution occurring along the axial and anterior/posterior directions. Average resultant drag force was 20% smaller for the crossed configurations. Maximum drag force orientation varied from 1.4° to 51°. Drag force angle varied from 1° to 5° during one cardiac cycle. 44% to 62% of the resultant force acted along the proximal centerline where SG migration is most likely to occur. The clinician's decision for SG positioning may be a critical parameter, and should be considered prior to surgery. All crossed SG devices had an increased spiral flow effect along the distal legs with reductions in drag forces.
© 2016 IPEM. Published by Elsevier Ltd. All rights reserved.

1. Introduction

Endovascular aneurysm repair (EVAR) by stent-graft (SG) devices is an effective alternative to conventional open repair for the treatment of abdominal aortic aneurysms (AAA) [1–4]. Over-the-wire techniques are used to deliver and deploy SG devices through the femoral artery to the abdominal region in attempt to shield the weakened AAA wall from the blood flow and pressure [5–6]. EVAR has less traumatic effects when compared with conventional surgical repair due to its minimally invasive nature [7]. Several post-operative complications are reported after the first year which includes SG migration, endoleaks, thrombus formation, endotension and device failure [8-12]. Several numerical studies have assessed the drag force effect along idealized [13], patient-specific [14-19] bifurcated SGs, while others examined the hemodynamics along non-crossed [15,20,21], crossed [20,22], blended taper [23] and custom made [24] SGs.

There can be a wide variety of positioning techniques for SG devices. Crossing of the graft limbs by the so called ballerina position reduces the effects of proximal neck angulation which may avoid endoleaks [25] and thrombosis due to graft kinking, which assists cannulation [22]. These positioning methods depend on the tortuosity of the vessels, in which the choice of rotating the graft limbs is decided upon by the surgeon. The crossing or non-crossing of graft limbs for bifurcated SG devices has not being totally accessed in terms of the blood flow effects and geometrical parameters. This study computationally assessed the hemodynamic and geometrical effects of eight patient-specific SG devices for crossed ($n=4$), non-crossed ($n=4$) and pre-operative ($n=4$) cases.

2. Methods

2.1. Geometries

Anonymized post-operative bifurcated SG devices for the treatment of AAAs ($n=8$) and pre-operative ($n=4$) computed tomography (CT) images were obtained in DICOM format from the Midwestern Regional Hospital, Limerick, Ireland, St. James Hospital, Dublin, Ireland and McGowan Institute for Regenerative Medicine,

* Corresponding author. Fax: +353 91758413.
E-mail address: liam.morris@gmit.ie (L. Morris).

http://dx.doi.org/10.1016/j.medengphy.2016.09.011
1350-4533/© 2016 IPEM. Published by Elsevier Ltd. All rights reserved.

Please cite this article as: F. Stefanov et al., A computational assessment of the hemodynamic effects of crossed and non-crossed bifurcated stent-graft devices for the treatment of abdominal aortic aneurysms, Medical Engineering and Physics (2016), http://dx.doi.org/10.1016/j.medengphy.2016.09.011

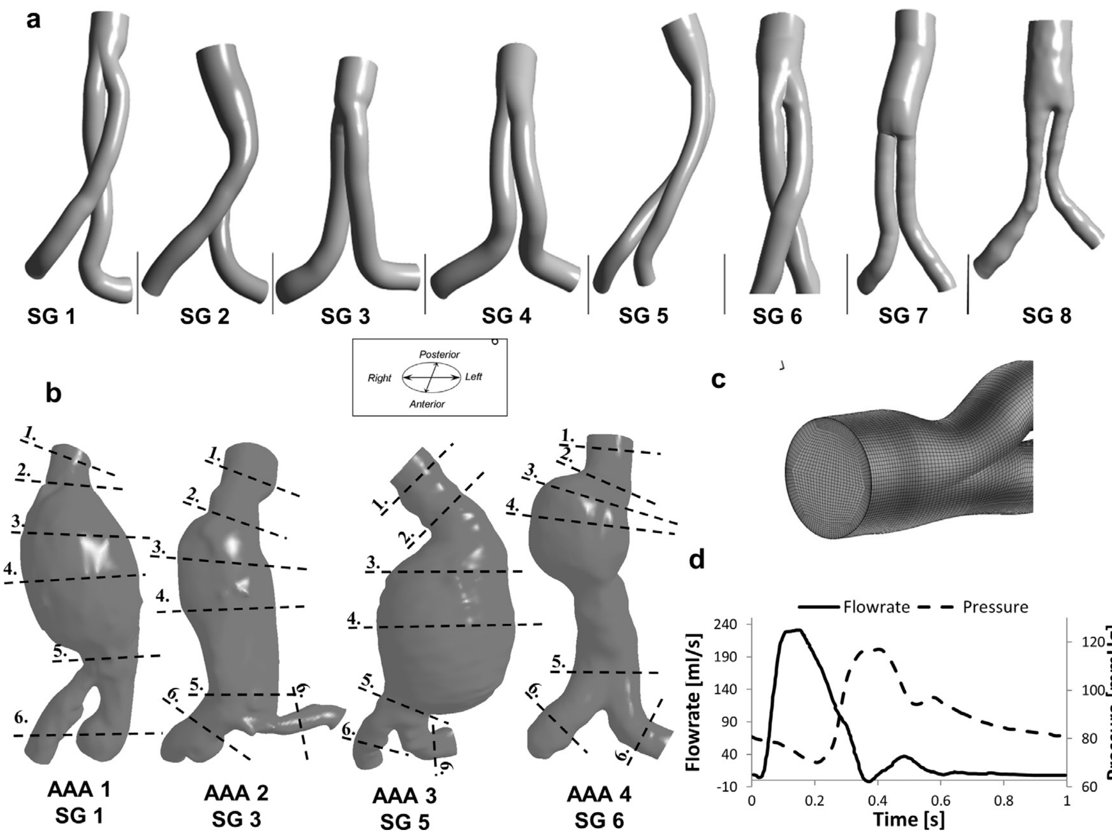

Fig. 1. (a) Eight patient-specific stent-graft geometries. (b) Four patient-specific pre-operative abdominal aortic aneurysm geometries. (C) O'grid structured mesh. (d) Imposed inlet flow rate (Nichols and O'Rourke, 1990) and outlet pressure (Di Martino et al., 2001) waveforms.

Table 1
Geometric measurements for all eight SG devices. C – crossed leg configuration and NC – non-crossed leg configuration.

Type and location	SG1	SG2	SG3	SG4	SG5	SG6	SG7	SG8
Proximal neck diameter (mm)	22.0	24.0	27.0	25.0	24.3	24.3	24.7	28.0
Distal left leg diameter (mm)	17.4	16.0	15.0	15.0	15.2	14.3	12.2	10.6
Distal right leg diameter (mm)	18.5	15.2	16.0	15.8	16.4	14.1	12.3	12.8
Proximal length (mm)	32.2	55.9	23.2	33.9	33.9	38.5	70.1	40.3
Left leg length (mm)	133.7	106.5	119.6	137.5	95.0	95	92.3	103.8
Right leg length (mm)	153.4	101.8	109.5	127.5	91.1	91.1	93.1	110.9
Leg angle at iliac bifurcation: αi (°)	36	54	62	68	40	43	58	64
Proximal anterior/posterior neck angle: βp (°)	21.3	21	9.8	56	13	7.8	7	18
Proximal lateral neck angle: γ (°)	26.5	30	14.3	5	62	33	9	5.5
Configuration	C	C	NC	NC	C	C	NC	NC

Pittsburgh, USA. The CT scan parameters had a slice thickness of 2.5 mm, resolution of 512 × 512 pixels and a pixel size of 0.7159 mm. Three-dimensional (3D) smoothed models enclosed by triangulated fitted surfaces were generated from the DICOM files by thresholding and smoothing techniques within the image segmentation software Mimics (Materialise, Mimics v14.0, Belgium) and exported as a binary Standard Tessellation Language (STL) format (Fig. 1(a) and (b)). Fig. 1a shows four conventional non-crossed (NC) and four crossed (C) leg SG configurations. Fig. 1b shows four selected pre-operative AAAs for SGs 1, 3, 5 and 6. Table 1 summarizes the geometrical characteristics for the four non-crossed and crossed configurations. The diameters of the proximal neck, left and right distal legs varied from (22.0–28.0 mm), (10.6–17.4 mm) and (12.3–18.5 mm) respectively. The limb lengths varied from (23–70 mm), (92–138 mm) and (91–153 mm) for the proximal end, left and right legs respectively. Also, there were angular variations of (36°–68°), (7°–56°) and (5°–30°) for the iliac limbs, proximal anterior/posterior and proximal lateral neck angles, respectively.

2.2. Numerical modeling

All the models, in binary STL format, were meshed by a structured multi-block O-grid within ICEM (Ansys ICEM, v.13.0) to generate the fluid domain (Fig. 1c). 300,000 elements were applied for each model. This grid density was shown previously by the authors to have mesh independence for velocity and wall shear stress values with less than a 2% change between successive meshes [20,23]. The blood was assumed to be incompressible, homogeneous and non-Newtonian fluid with a density of 1050 kg/m^3 [26], and a dynamic viscosity described by the Carreau–Yasuda shear thinning model as shown in Eq. (1).

$$\frac{\mu - \mu_\infty}{\mu_0 - \mu_\infty} = [1 + (\lambda \cdot \dot{\gamma})^a]^{(n-1)/a} \tag{1}$$

where $\dot{\gamma}$ denotes the scalar shear rate, $\mu_0 = 0.16$ Pa s, $\mu_\infty = 0.0035$ Pa s, $\lambda = 8.2$ s, $n = 0.2128$, and $a = 0.64$ [27,28]. Fig. 1d shows the inlet flow rate as found by a catheter-tip electromagnetic flow transducer [29] and outlet pressure waveform as obtained by an electromagnetic catheter transducer [30] for a

Download English Version:

https://daneshyari.com/en/article/5032776

Download Persian Version:

https://daneshyari.com/article/5032776

Daneshyari.com